Geofísica Internacional (1996), Vol. 35, Num. 1, pp. 41-50

Maximum seismic depth versus thermal parameter of subducted slab: application to deep earthquakes in Chile and Bolivia

A. Gorbatov[1], V. Kostoglodov[1] and E. Burov[2]
[1] *Instituto de Geofísica, Universidad Nacional Autónoma de México, México D.F., México.*
[2] *Institut de Physique du Globe de Paris, Paris, France.*

Received: April 28, 1995; accepted: November 13, 1995.

RESUMEN

La relación de la profundidad sísmica máxima (D_m) contra el parámetro térmico de la placa subducida (φ), se determina por medio de la edad de la litosfera subducida (A) y la componente vertical de velocidad de subducción ($V_\perp$), en perfiles de sismicidad perpendiculares a las zonas de subducción de México, Chile, Kamchatka, Kuriles, Japón, Sumatra, Nuevas Hebridas y Aleutianas. La parte cuasi-lineal de la relación ($D_m \leq 240$ km, y $\varphi \leq 20\text{x}10^2$ km), corresponde a la placa que se subduce lentamente y es relativamente joven; en general coincide con la "temperatura crítica" modelo de los eventos profundos. Para el rango de $\varphi > 20\text{x}10^2$ km, cual corresponde a la placa subducida relativamente vieja y que se subduce rápidamente, la relación $D_m = f(\varphi)$ no es lineal. La curva empírica $D_m = f(\varphi)$ tiene una mesa en el rango de $20\text{x}10^2$ km $< \varphi < 35\text{x}10^2$ km por la transición equilibrada de la fase Ol-Sp a la profundidad sísmica máxima, D_m. Los modelos que consideran la transición metastable de la fase Ol-Sp como causante de la sismisidad profunda no pueden ser analizados con los resultados del presente estudio. Los eventos profundos de la zona de subducción de Chile y el evento fuerte $M_w = 8.2$, junio 9, 1994 en Bolivia, han sido analizados usando la dependencia estándar $D_m = f(\varphi)$. Los eventos profundos de Chile al sur de 26°S caen fuera de la curva de $D_m = f(\varphi)$ lo que permite identificarlos como procedentes del fragmento desacoplado de la placa subducida. Los otros eventos, incluyendo el evento de Bolivia, están dentro del rango de los errores estimados. Este resultado indica que los eventos chilenos de la parte norte no necesariamente pertenecen a la parte desacoplada del slab y el evento de Bolivia probablemente ocurrió en el borde de la parte norte más vieja y profunda de la placa de Nazca.

PALABRAS CLAVE: Sismisidad profunda, subducción, estructura térmica del slab, transición de fase Ol-Sp, junio 9, 1994 terremoto de Bolivia.

ABSTRACT

The maximum seismic depth (D_m) depends on the thermal parameter of the descending slab (φ), which is a product of the age of the subducted lithosphere (A) and the vertical component of convergence rate ($V_\perp$). We analyze seismicity profiles across the subduction zones of Mexico, Chile, Kamchatka, Kuriles, Japan, Sumatra, New Hebrides and Aleutians. The quasi-linear part of the dependence ($D_m \leq 240$ km, and $\varphi \leq 20\text{x}10^2$ km) corresponds to relatively young and slowly descending slab and is in general agreement with the "critical temperature" models of deep earthquakes. For $\varphi > 20\text{x}10^2$ km, which corresponds to the relatively older lithosphere subducting at a higher rate, the $D_m = f(\varphi)$ dependence is essentially nonlinear. The flattening of the empirical $D_m = f(\varphi)$ curve in the range of $20\text{x}10^2$ km $< \varphi < 35\text{x}10^2$ km is found to be a direct indication of the influence of the equilibrium Ol-Sp phase transition on D_m. Models invoking the metastable Ol-Sp phase transition as a mechanism which controls the deepest seismicity can not be constrained by the results of this study. Deep focus earthquakes of the Chilean subduction zone and the strong event of June 9, 1994 in Bolivia ($M_w = 8.2$), were analyzed using the general standard dependence $D_m = f(\varphi)$. A group of Chilean deep events south of 26°S has occurred inside the detached fragment of the subducted slab. D_m values corresponding to these deep events lie outside $D_m = f(\varphi)$ curve. All other events, including the Bolivian earthquake, fit the curve within the uncertainty estimate. Thus the northern group of Chilean events does not necessarily pertain to the detached slab, and the Bolivian earthquake probably occurred at the northernmost deep edge of the oldest segment of the subducted Nazca plate.

KEY WORDS: Deep seismicity, subduction, thermal structure of the slab, Ol-Sp phase transition, June 9, 1994 Bolivian earthquake.

INTRODUCTION

A conductive heating model (McKenzie, 1969) of the lithospheric slab descending into the isothermal mantle has been fairly successful at explaining the variation of the maximum depth of seismicity, D_m, along the Tonga-Kermadec trench (Sykes, 1966). D_m is the maximum depth to which a particular "critical" isotherm ($T_{cr} \approx 800$°C) within the subducting slab has penetrated into the mantle. Below the depth D_m the material comprising the subducted lithospheric slab exhibits temperatures greater than T_{cr}, and loses its ability to generate earthquakes. According to the model, D_m should be proportional to the product of the convergence rate, V, and the age, A, of the lithosphere. For a slab which is subducting in the non-isothermal mantle this relation is valid only for a dip angle α=90° (vertically subducting slab).

The model is also valid for $\alpha \leq 90°$ if the mantle exhibits a temperature distribution which is close to adiabatic (McKenzie, 1970). In this case a general relation for a particular potential temperature T'_{cr} is

$$L_m \propto VA, \quad (1)$$

where L_m is the maximum length of downdip seismic activity along the subducting slab. A test of relation (1) with data for different subduction zones shows that the relation is approximately linear for L_m up to 600 km, where $VA < 40x10^2$ km (Molnar *et al.*, 1979; Shiono and Sugi, 1985).

For a vertical temperature gradient in the mantle, the slab heating should depend mostly on the vertical component of the convergence rate, $V_\perp = V\sin\alpha$, instead of the total scalar value of V. Two subduction zones with the same values of V and A but with different dip angles $\alpha_1 < \alpha_2$ would have different lengths of seismic activity, $L_{m1} > L_{m2}$, because adiabatic heating should raise the temperature inside the steeper slab (α_2) as compared to the shallow one. It is worthwhile to reformulate relation (1) in terms of an explicit function of the product $V_\perp A$ (Kostoglodov, 1989); specifically

$$D_m \propto L_m \sin\alpha = kVA\sin\alpha + d = k\varphi + d, \quad (2)$$

where $\varphi = VA\sin\alpha$ is called the "thermal parameter" of the descending lithospheric slab (Kirby *et al.*, 1991), and k and d are constants. Relation (2) is valid if temperature (T_{cr}) alone is controlling the occurrence of deep earthquakes.

It has been shown that relation (2) agrees roughly with the observed $D_m \leq$ 250-300 km, in the range $\varphi = 0$ to $20x10^2$ km (Kostoglodov, 1989). In this range, earthquakes occurring at depths less than 300 km inside the subducting slab are believed to be generated by brittle failure and frictional sliding along the fault surface. That occurs probably when some minerals, such as serpentine, dehydrate and release liquid water (Meade and Jeanloz, 1991). A review of the probable mechanisms and the physical factor controlling deep seismicity may be found in Frohlich (1989) and Lay (1994).

For $\varphi > 20x10^2$ km the relationship $D_m = f(\varphi)$ is essentially non-linear and therefore the "critical temperature" model does not seem to be applicable. Using a data set of D_m, V and A to analyze the $D_m = f(\varphi)$ dependence, Kostoglodov (1989) suggested that the observed deviation of D_m vs. φ from the expected linear dependence may be explained by the influence of the Ol-Sp phase transition, and particularly by the metastable Ol-Sp transition, on the physical mechanism of deep earthquakes. A study of Kalinin and Rodkin (1982) and other recent studies (Green and Burnley, 1989; Green *et al.*, 1990; Kirby *et al.*, 1991; Green, 1994) indicate that earthquakes occurring at depths greater than 300 km may be associated with solid-state phase transitions, predominantly in metastable olivine (for example, transformational faulting, anticrack-associated faulting, etc.). Kirby *et al.* (1991) argued that the distinctive deviation from linearity of $D_m = f(\varphi)$ for relatively old and rapidly subducting lithosphere may favor the transformational faulting model based on the results of laboratory experiments with phase transition in ice.

The empirical relation $D_m = f(\varphi)$ was previously evaluated with the broadly averaged subduction parameters such as V and A that were used in the previous studies (Kostoglodov, 1985; Kirby *et al.*, 1991), but which introduced large uncertainties. Molnar *et al.* (1979) and Wortel (1982) demonstrated that $T_{cr} \neq$ const, on the contrary, it increases with depth. Thus both temperature and pressure may affect the seismicity cutoff in the subducting slab. Recent numerical modeling of Spencer (1994) revealed that the calculated relationship between slab length, L_m, as defined by temperature threshold $T_{cr} = 650°C$, and the product VA (see eq. (1)) is not linear. Unfortunately, the accuracy of previous empirical relationships is not sufficient to resolve the nonlinearity.

Whatever the actual physical mechanism of intermediate and deep earthquakes may be, the accurate empirical relation $D_m = f(\varphi)$ would be of great interest for the study of deep seismicity and tectonics of subduction zones. For example, relation (2) can be applied to subduction zones with $D_m < 250$ km but unknown convergence velocity or age of subducted lithosphere in order to assess these parameters (Kostoglodov and Bandy, 1995), Gorbatov *et al.* 1995).

The main objectives of this study are: (1) To accurately achieve the empirical dependence $D_m = f(\varphi)$ through detailed analysis of subduction parameters in Mexico, Chile, Kamchatka, Kuriles, Japan, Sumatra, New Hebrides and Aleutian subduction zones. (2) To analyze the consistency of the obtained empirical relation with the recent models of slab heating in order to assess a cutoff temperature for the intermediate and deep focus earthquakes. (3) To demonstrate an application of the empirical dependence for the analysis of deep earthquakes in Chile, and for the Bolivian earthquake of June 9, 1994.

DATA

To estimate D_m and α we use cross-sections of the Wadati-Benioff seismic zones in Mexico, Chile, Kamchatka, Kuriles, Japan, Sumatra, New Hebrides and Aleutians. For the Kamchatka subduction zone the catalog of the regional seismic network (1962-1994) is used. New seismicity profiles across the subduction zone of Mexico are taken from Pardo and Suárez (1995). Regional seismicity data of Japan are used from Zhao *et al.* (1992). For the rest of the subduction zones, the data from the ISC Bulletin (NEIC CD 1964 -1987) are used. The following criterion is used for the selection of the subduction zones and seismicity profiles for this study: (a) subduction zones with updated age estimates (by using linear magnetic anomalies) are preferred, (b) the subduction regime should be unperturbed, so the cross-sections must be chosen in sections of subduction zone which do not contain prominent subducted bathymetric features. The cross-sections are selected mostly parallel to the vector of subduction velocity to facilitate the assessment of D_m and α; otherwise a special correction (Shiono and Sugi, 1985) for the angle between the direction of profile and vector V is applied. The value of D_m is taken as the depth of the deepest event along the cross-section. An average dip angle, α, is calculated as (D_m/L_s) where L_s is the projection of L_m on the Earth's surface.

The uncertainties associated with maximum seismic depths were estimated for each profile as the separation between the deepest and next deepest event. The uncertainty in the angle of subduction was determined from the uncertainty in D_m. This averaged uncertainty is not higher than approximately ±1.5°-2.0°.

The convergence rates and the associated uncertainties were calculated from the NUVEL 1A model (DeMets *et al.*, 1994) at the location where the true path of the point corresponding to D_m intersects the trench. The error in V estimates depends on each pair of plates sharing the subduction boundary (DeMets *et al.*, 1994) and in this case is less than 3.5%.

The main difficulties usually arise in estimating the age of the subducted lithosphere, because A in equations (1, 2) is the age of that segment of the lithospheric plate now located at depth D_m when it first started to subduct. To estimate this age we use the relation (Shiono and Sugi, 1985)

$$A = A_t + L_m / V_s - L_m / V \ , \qquad (3)$$

where A_t is the age of the lithosphere at the trench. Equation (3) assumes that the half spreading rate, V_s, during the time interval A_t to L_m/V_s was constant. A pick up error in A_t is usually less then 1 m.y. The errors in A and φ are calculated using the error propagation equation (e.g., Bevington, 1969) applied to (3) and (2) respectively. In addition to the random errors, some indefinite systematic error may be involved in φ estimates related to the assumption that V_s = const.

Table 1 summarizes the estimates of D_m and φ together with the uncertainties. The estimates of A, V, α, the coordinates at the trench and the azimuth of each cross-section are also included.

DEPENDENCE OF D_m ON φ

Figure 1 represents a plot of $D_m=f(\varphi)$ based on the data from Table 1. An important feature of this plot is a significantly reduced scatter of D_m and smaller errors of φ esti–

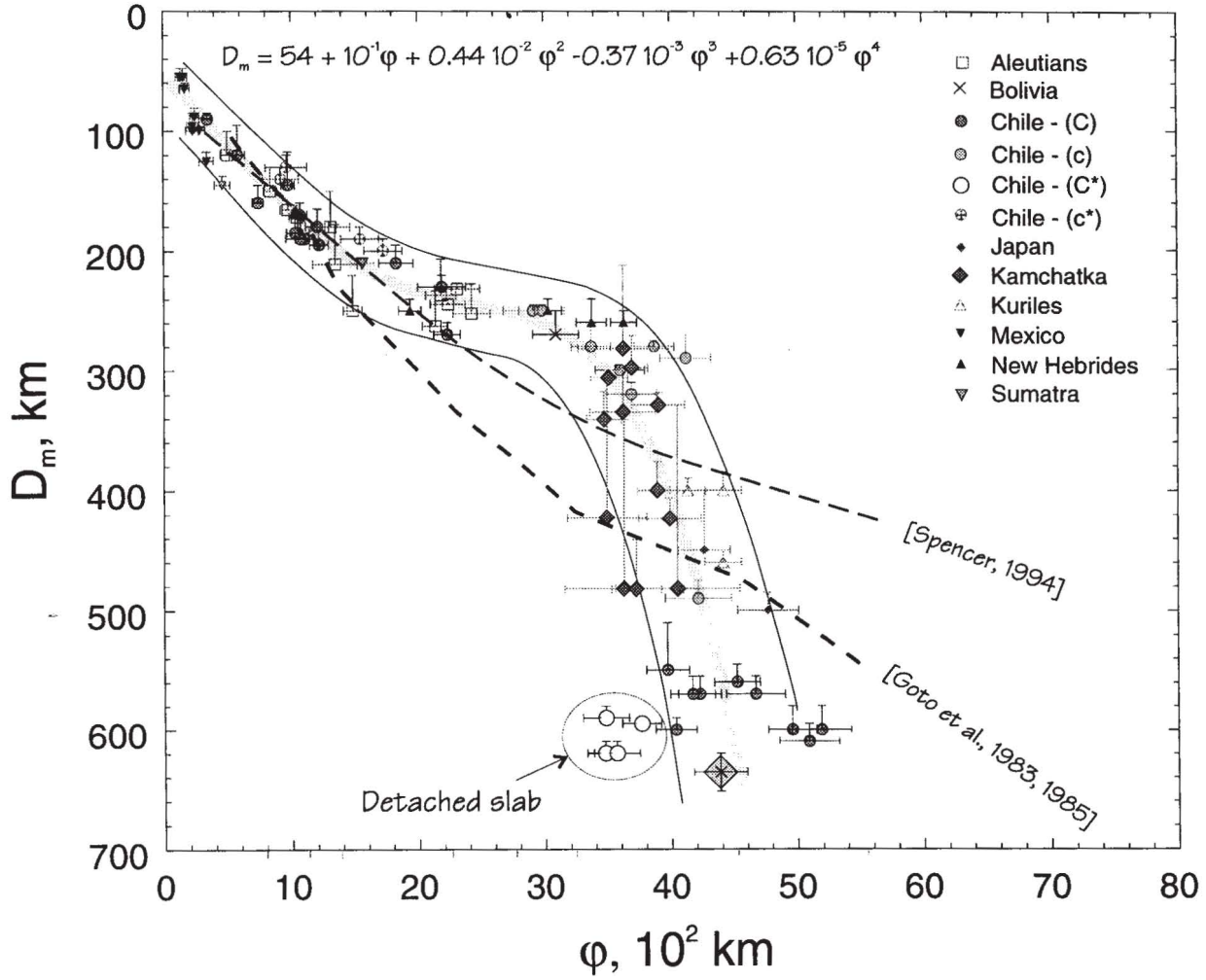

Fig. 1. Plot of the observed D_m against the thermal parameter of descending slab, φ, based on the data from Table 1. Heavy gray curve is the best-fitting polynomial $D_m=f(\varphi)$ and thin curves are 95% confidence bounds. Long dashed curves are the $D_m=f(\varphi)$ dependencies assessed from Goto *et al.* (1983, 1985) and from Spencer (1994) for T_{cr}=650°C. The last one is adjusted to the empirical data (120 km shift for the thickness of the continental lithosphere in the model). The Bolivian June 9, 1994 earthquake is shown as a large shaded diamond. Legend: Chile-(C*) deep events inside the detached slab; Chile-(c*) the same Chilean cross-sections but without the deep detached slab events; Chile-(c) Chilean cross-sections with D'_m - max depth ahead of the aseismic gap.

Table 1

Summary of parameters

No.[a]	Lat °N	Lon °E	Az deg.	V^b mm yr	θ deg.	A^c m.y.	α deg.	D_m km	ΔD_m km	φ km	Δφ km
A1	51.6	172.7	27	73	317	36	35	120	20	5.0	0.5
A2	50.5	177.8	17	73	318	44	36	166	5	9.8	0.6
A3	50.2	-179.6	4	72	320	62	44	245	5	22.4	1.4
A4	50.3	-177.4	357	71	320	63	43	253	25	24.2	1.5
A5	50.7	-174.6	352	70	322	63	37	232	5	23.1	1.8
A6	50.9	-171.2	347	68	324	51	42	263	30	21.4	1.0
A7	51.5	-168.3	328	67	325	51	40	237	30	21.8	1.2
A8	55.0	-154.5	328	59	335	52	25	180	30	13.1	1.5
A9	55.4	-153.4	328	58	336	52	26	211	33	13.5	1.8
A10	55.8	-152.4	328	58	337	52	30	250	30	14.9	0.7
A11	56.3	-151.2	328	57	338	48	23	172	10	10.5	0.6
A12	57.4	-148.8	328	55	341	46	20	150	20	8.4	0.5
B1	-18.5	-72.5	47	77	81	109	39	636	10	43.9	1.4
b	-18.5	-72.5	47	77	81	92	39	270	10	30.9	1.4
C1	-42.0	-75.5	74	80	80	15	14	90	5	3.4	0.4
C2	-41.0	-75.3	74	80	80	20	18	120	25	5.8	0.6
C3	-40.0	-75.1	74	80	80	20	22	160	15	7.4	0.4
C4	-39.0	-75.0	74	80	79	25	25	185	13	10.3	0.6
C5	-38.0	-74.9	74	80	79	31	19	145	28	9.8	0.5
C6	-37.0	-74.7	74	80	79	32	23	195	13	12.1	0.7
C7	-36.0	-74.3	74	80	79	34	19	170	10	10.7	0.6
C8	-35.0	-73.9	74	80	79	41	19	185	13	10.5	0.9
C9	-34.0	-73.3	74	80	79	47	17	190	5	11.0	0.7
C10	-33.0	-72.9	74	80	78	55	14	190	20	10.8	1.2
C11	-32.0	-72.7	74	80	78	62	14	180	15	12.1	0.9
C12	-31.5	-72.8	74	80	78	64	21	210	15	18.3	1.4
C13	-27.0	-72.0	74	80	78	92	33	600	10	40.4	1.6
C14	-26.0	-71.7	74	80	78	98	33	570	15	42.3	1.7
C15	-25.0	-71.5	74	79	78	103	29	550	40	39.8	1.7
C16	-24.0	-71.5	74	79	78	108	29	570	15	41.7	1.8
C17	-23.0	-71.4	74	79	78	108	32	560	15	45.3	1.8
C18	-22.3	-71.3	74	78	77	111	33	570	15	46.7	2.3
C19	-21.0	-71.4	74	78	77	111	36	610	15	50.9	2.4
C20	-20.0	-71.6	74	78	77	111	37	600	20	51.9	2.4
C21	-19.0	-72.7	74	77	78	112	35	600	20	49.6	1.9
C22	-17.4	-74.4	74	77	79	73	23	230	10	21.9	1.9
C23	-16.5	-75.4	74	77	79	67	26	270	10	22.3	1.1
c14	-26.0	-71.7	74	80	78	85	26	250	5	29.8	1.8
c15	-25.0	-71.5	74	79	78	87	25	250	5	29.1	2.3
c16	-24.0	-71.5	74	79	78	94	29	300	5	36.0	2.0
c17	-23.0	-71.4	74	79	78	97	29	320	10	36.9	2.0
c18	-22.3	-71.3	74	78	77	102	32	490	15	42.2	2.6
c19	-21.0	-71.4	74	78	77	97	33	290	20	41.2	2.0
c20	-20.0	-71.6	74	78	77	99	30	280	5	38.7	1.6
c21	-19.0	-72.7	74	77	78	102	25	280	20	33.7	1.6
C1*	-31.0	-72.7	74	80	78	81	33	620	10	34.8	1.4
C2*	-30.2	-72.6	74	80	78	83	33	620	10	35.7	1.8
C3*	-29.3	-72.6	74	80	78	83	32	590	10	34.8	1.8
C4*	-28.4	-72.5	74	80	78	89	32	595	5	37.7	1.6
c1*	-31.0	-72.7	74	80	78	66	10	140	10	9.2	1.4
c2*	-30.2	-72.6	74	80	78	70	16	190	10	15.4	1.5
c3*	-29.3	-72.6	74	80	78	70	18	200	10	17.3	1.5
c4*	-28.4	-72.5	74	80	78	77	9	130	10	9.6	1.6
Jp1	41.4	145.5	324	83	117	103	34	450	50	42.7	2.1
Jp2	35.3	142.4	304	93	292	104	31	500	15	47.7	2.4
K1	50.2	159.4	302	78	306	67	45	482	41	37.3	2.0
K2	50.6	159.8	302	77	306	72	44	400	24	38.9	1.6
K3	50.9	160.2	302	77	307	69	49	482	153	40.6	5.0
K4	51.3	160.6	302	77	307	66	45	482	141	36.3	5.0
K5	51.7	160.8	302	77	307	71	47	424	18	40.0	2.5
K6	52.1	161.1	302	76	307	64	53	329	10	39.0	2.1
K7	52.8	161.9	302	76	308	65	45	423	117	35.0	3.2
K8	53.1	162.4	302	76	309	67	43	341	23	34.7	1.4
K9	53.5	162.8	302	75	309	67	46	335	35	36.2	2.6
K10	53.8	163.0	302	75	309	69	43	306	6	35.1	1.5
K11	54.2	163.2	302	75	309	70	44	282	70	36.3	3.6
K12	54.5	163.4	302	75	309	70	45	298	27	36.9	1.3
Ku1	44.5	150.0	320	82	300	82	45	460	10	44.2	1.5
Ku2	44.0	149.0	320	82	300	85	43	400	15	44.2	1.5
Ku3	43.3	148.0	320	82	299	84	40	400	10	41.4	1.4
M1	15.3	-96.0	33	67	33	16	25	145	8	4.6	0.4
M2	15.4	-97.0	34	65	34	16	20	125	8	3.4	0.4
M3	15.6	-98.0	35	62	35	15	15	100	15	2.3	0.3
M4	15.9	-99.0	35	60	35	14	17	96	9	2.3	0.3
M5	16.2	-100.0	35	58	35	13	13	65	5	1.7	0.2
M6	16.5	-101.0	36	55	36	12	12	55	8	1.3	0.2
M7	16.8	-102.0	36	53	36	13	13	55	8	1.5	0.2
M8	17.3	-103.0	36	50	36	13	26	99	10	2.9	0.3
M9	17.9	-103.9	36	47	36	13	25	88	8	2.5	0.3
N1	-12.0	165.7	75	91	80	24	63	250	10	19.4	0.9
N2	-14.8	166.6	75	87	80	45	70	260	10	36.3	1.0
N3	-15.6	166.8	75	85	80	44	65	260	20	33.7	1.2
N4	-17.6	167.1	75	82	80	45	55	250	10	30.3	1.1
Su1	-4.5	100.0	50	68	19	53	30	210	15	15.6	0.9

The column abbreviations are: Lat-Latitude, Lon-Longitude (coordinates of the intersection point between the profile and the trench), Az - Azimuth of the cross-section, θ - Azimuth of the convergence velocity, ΔD_m and Δφ uncertainties in the estimates of D_m and φ respectively.

a Abbreviations are: A- Aleutians; B - Bolivia; C- Chile; C*- Chile, profiles for the detached slab; Jp -Japan; Su - Sumatra; K - Kamchatka; Ku - Kuriles; M - Mexico; N - New Hebrides; b, c, c* - Bolivia and Chile (D'_m - max depth ahead of the aseismic gap).

b Derived from DeMets *et al.* (1994).

c Aleutians: Atwater (1989); Bolivia, Chile: Mayes *et al.* (1990); Japan: Nakanishi *et al.* (1992); Sumatra: Neprochnov *et al.* (1979), Mueller *et al.* (1993); Kamchatka: Renkin and Sclater (1988); Kuriles: Larson *et al.* (1985), Nakanishi *et al.* (1992); Mexico: Mammerickx and Klitgord (1982); New Hebrides: Larue *et al.* (1977), Circum-Pacific Council... (1981), Weissel *et al.* (1982).

mates in comparison with the previous studies (Kostoglodov, 1989; Kirby *et al.*, 1991). This permits one to approximate the general empirical relationship with a simple curve. For example, the best-fit polynomial curve shown in Figure 1 has the coefficients $\mathbf{a}(a_0,a_1,...,a_4) = (54, 10^{-1}, 0.44\times10^{-2}, -0.37\times10^{-3}, 0.63\times10^{-5})$.

To compare obtained empirical dependence with the modeled minimum temperature distribution in the slab, the following procedure is used. A set of coldest geotherms inside the subducting lithosphere with different values of φ is found from the results of numerical modeling by Goto *et al.*, (1983, 1985). Each of these geotherms represents on the P-T diagram (Figure 2) the distribution of minimum temperature within the slab as a function of depth or pressure in the mantle. Using the value of φ of each modeled geotherm, the D_m estimate and its uncertainty from the empirical dependence $D_m=f(\varphi)$ in Figure 1 are superimposed on that geotherm in Figure 2. The range of empirical estimates of D_m in Figure 2 (shaded curved band) represents the P-T conditions of the seismicity cutoff in the subducting slab for the model of Goto *et al.*, (1983, 1985).

Down to $D_m \approx 240$ km and up to $\phi \approx (15\text{-}20)\times10^2$ km the critical temperature changes gradually from ~ 700°C to ~600°C (gray circles in Figure 2). These cutoff conditions of the model correspond to a relatively young and slowly descending slab. They differ from the results of Molnar *et al.* (1979), where T_{cr} was rising with depth. The model $D_m=f(\varphi)$ curve for T_{cr} = 650°C was obtained from the geotherms presented in Figure 2 and plotted in Figure 1 as a dashed curve (Goto *et al.*, 1983, 1985). As can be seen from Figure 1, the model does not fit well the empirical $D_m=f(\varphi)$ relation for the constant T_{cr}.

A better approximation for the empirical $D_m=f(\varphi)$ relation in its quasi-linear section (D_m < 240 km) is the model of Spencer (1994). In this model the controlling mechanisms of the seismicity cutoff are the drop of compressive slab strength below 10^{13} N/m, and the increase of slab core temperature of more than 650°C. Above this temperature the calculated slab strength is defined entirely by disloca–

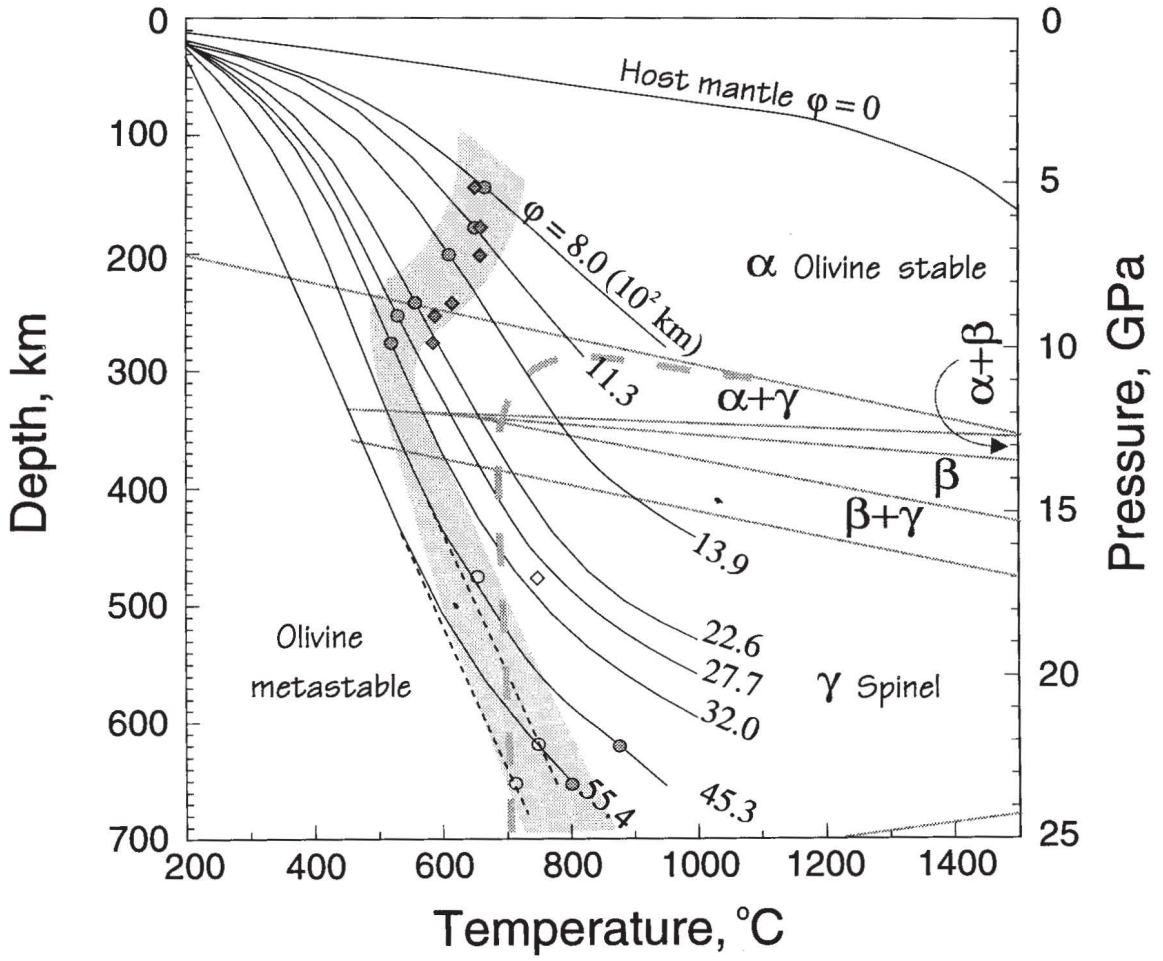

Fig. 2. Phase diagram and coldest geotherms of the subducting slab (lines annotated with the values of φ) from the thermal model of Goto *et al.* (1983, 1985). The circles and diamonds indicate D_m for each geotherm with its particular value of φ for the models of Goto *et al.* (1983, 1985) and Spencer (1994). Open symbols denote interpolated values. Straight lines are equilibrium transitions for different phases (α→β→ γ) of the composition $(Mg_{0.89} - Fe_{0.11})_2 SiO_4$ (Akaogi *et al.*, 1989). Shaded curved band represents average P-T conditions of seismicity cutoff in the subducting slab (model of Goto *et al.*, (1983, 1985)) with different values of φ. Gray long dashed curve is the expected kinetic phase boundary between the metastable and stable phases with the characteristic temperature T_{ch} ~700°C (Sung and Burns, 1976). Host mantle geotherm (φ = 0) (Von Herzen, 1967) used in the model of Goto *et al.*, (1983, 1985). Dashed black lines are coarse interpolations of the geotherms for φ = 45.3 and φ = 55.4 as if the slab in the model of Goto *et al.* (1983, 1985) were not heated from its bottom tip.

tion creep in olivine. The $D_m=f(\varphi)$ dependence from Spencer (1994), adjusted to the empirical data, is shown in Figure 1. This model for the temperature cutoff T_{cr} = 650°C is very close to the best-fitting polynomial curve only within the range of $\varphi < 20x10^2$ km.

The next range of φ from $20x10^2$ km to ~$35x10^2$ km (relatively older lithosphere subducting at a higher rate) is not related to further apparent increase of D_m. It approximately remains at the level of $D_m \approx 260$ km (Figure 1). For the model of Goto *et al.*, (1983, 1985) T_{cr} in that range of φ decreases even more, down to (550°C, and for the model of Spencer (1994) this decrease is somewhat less, T_{cr} ~600°C (Figure 2). The drop of T_{cr} may be interpreted by the influence of the Ol-Sp phase boundary which crosses the geotherms with $20x10^2$ km <φ< $35x10^2$ km approximately at a depth of 260 km (Figure 2). Neither of these models includes the effect of latent heat released by the Ol-Sp phase transition which should increase the temperature in the slab core by $\Delta T \approx 130$°C (e.g., Turcotte and Schubert, 1971). The geotherms roughly corrected for ΔT are presented in Figure 3. As can be seen this correction produces an increase of T_{cr} with depth (as well as with φ) which is physically more meaningful and consistent with the conclusions of previous studies (e.g., Molnar *et al.*, 1979, Wortel, 1982).

The drastic increase of D_m from ~ 260 km to > 600 km in the narrow range of $35x10^2$ km <φ< $45x10^2$ km (Figure 1) has been considered in favor of the models invoking the metastable Ol-Sp phase transition as a mechanism for the deepest seismicity (e.g., Kostoglodov, 1989, Kirby *et al.*, 1991). Unfortunately, the large uncertainty in D_m and φ in this range and upward deflection of the geotherms for D_m >

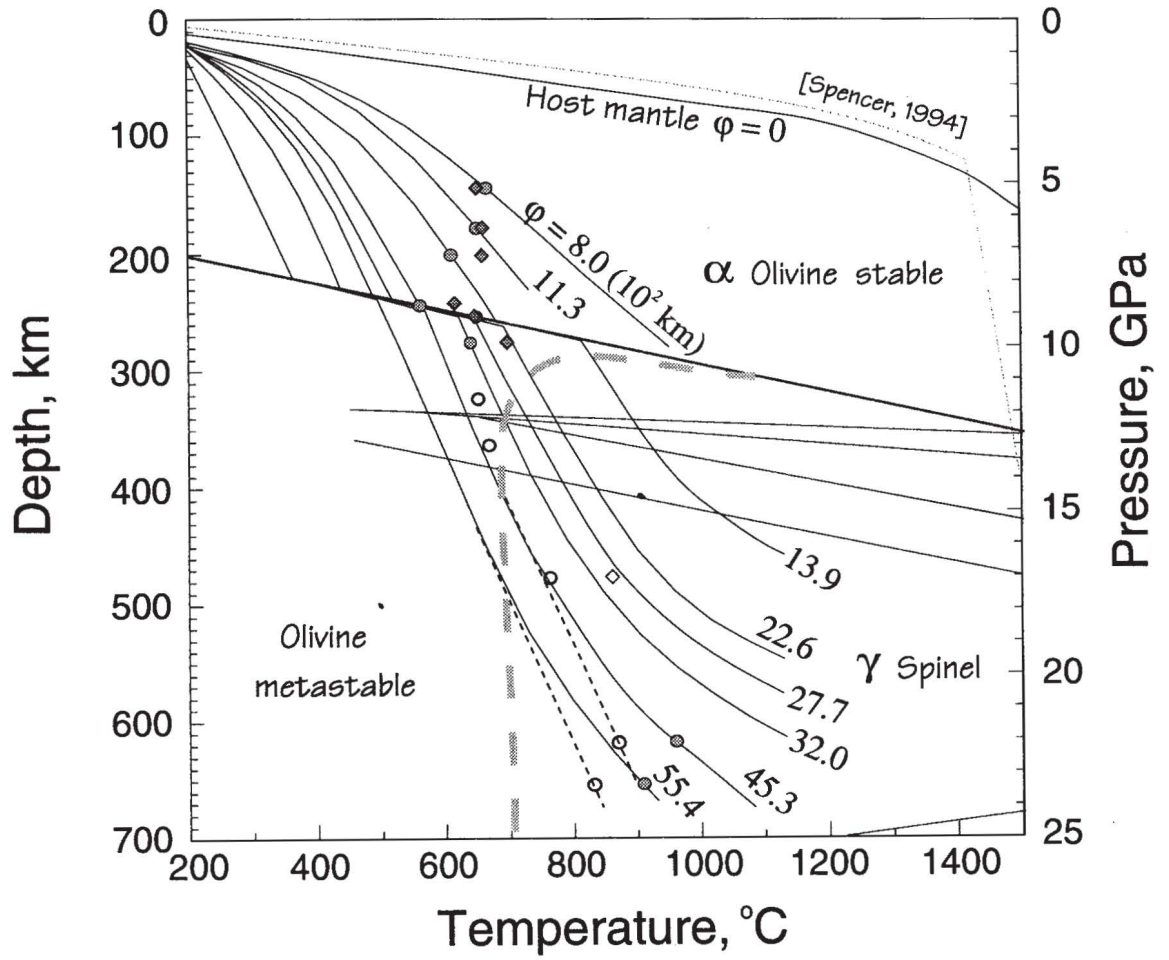

Fig. 3. Same as Figure 2, except the coldest geotherms are corrected for the latent heat effect of equilibrium Ol-Sp phase transition $\Delta T \approx 130°C$. The points of the maximum seismic depth, D_m, below the $\alpha+\gamma$ phase line are shifted by that correction. Open circles and diamond denote D_m corresponding to interpolated and extrapolated values of φ. Topmost dashed line is the mantle geotherm in the model of Spencer (1994).

450 km (as a result of the model inference, the sinking slab is heating from its downgoing tip (Goto *et al.*, 1983, 1985)) do not allow us to make this conclusion. The cutoff P-T conditions for observed values of D_m and φ are far beyond the hypothetical kinetic boundary between metastable olivine and stable spinel with its characteristic temperature $T_{ch} \sim 700°C$ (Sung and Burns, 1976) (Figures 2 and 3). New accurate data for other subduction zones and more adequate modeling (involving Ol-Sp equilibrium phase transition and metastable Ol-phase in cold slab core) are required in this range of the empirical dependence $D_m=f(\varphi)$.

Some convergent zones in the western Pacific with very old ($A>100$ my) subducting lithosphere (e.g., Mariana, Tonga, New Zealand) were not considered because the age estimates for these regions are not adequate to make a proper correction for A in equation (3). However, D_m does not change significantly (~600÷670 km) over a large range of $\varphi > 50 \times 10^2$ km (Kostoglodov, 1989; Kirby *et al.*, 1991).

DEEP EARTHQUAKES IN CHILE AND BOLIVIA

The empirical dependence $D_m=f(\varphi)$ (Figure 1) is applied to the deep seismicity in central Chile (south of 25°S) and to the Bolivian earthquake of June 9, 1994. Deep events of Chile north of 23°S and south of the Easter fracture zone apparently occurred within the oldest ($A > 80$ my) segment of the subducted Nazca plate (Kostoglodov, 1994) (Figure 4). The shape of seismicity cross-sections and new age estimates (Mayes *et al.*, 1990) do not require the slab detachment in this region (Engebretson and Kirby, 1992) to explain the maximum depth of seismicity. Based on that assumption, the cross-sections to the north of 23°S are used to constrain the $D_m=f(\varphi)$ dependence.

Because of a lack of intermediate depth seismicity in the cross-sections corresponding to the deep events located between 23°S and 26°S, it is not clear whether they pertain to the continuous or detached slab. On the $D_m=f(\varphi)$ plot

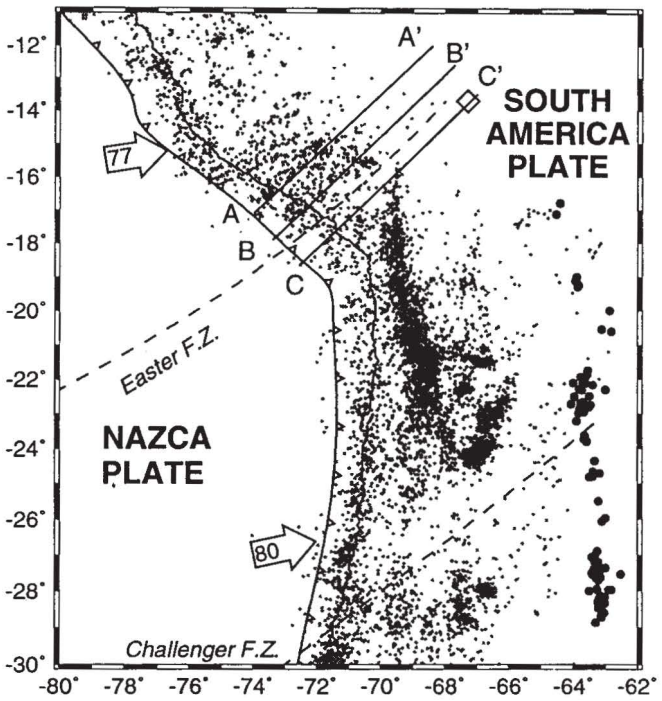

Fig. 4. Location map of cross-sections A-A', B-B' and C-C' for the Chilean subduction zone. Arrows show convergence rate in mm/yr (DeMets *et al.*, 1994). Gray dots are epicenters of earthquakes (ISC Bulletin, NEIC CD, from 1964 to 1987). Black circles indicate deep events, hypocentral depth > 500 km. Open diamond is the Bolivian event of June 9, 1994. See text for further explanation.

these events (c in Figure 1 and Table 1) are scattered around some average value of $\varphi \sim 45x10^2$ km and $D_m \sim 550$-600 km. The southernmost deep seismicity of the Chilean subduction zone (26°S-29°S, see Figure 4) is shifted from the general dependence curve to the lower $\varphi \sim 35x102$ km (Figure 1), and can be identified on the seismic cross sections as taking place within the detached fragment of the Nazca plate (e.g., Kostoglodov, 1994).

The $M_w = 8.2$ earthquake occurred on June 9, 1994 under Bolivia (e.g. Kirby *et al.*, 1995, Lundgren and Giardini, 1995). Most likely it belongs to the northernmost deep edge of the oldest segment of the subducted Nazca plate, just southeast of the extension of the Easter fracture zone (Figure 4). Cross-section C-C' of the Wadati-Benioff zone suggests (Figure 5) that this earthquake occurred within the unfragmented slab. A large aseismic gap (~300 km) exists along the subducting slab between the deepest events of the profile and the Bolivian earthquake, but the point corresponding to that event fits, within the error estimates, the general dependence $D_m=f(\varphi)$ (Figure 1).

It is interesting to note that for the smooth-shaped cross-sections with a seismic gap from D'_m to the deepest events D_m (such as profile C-C' in Figure 4) usually both points D'_m and D_m fit the dependence $D_m=f(\varphi)$. This is true for the Chilean cross-sections C14-C21 and C1*-C4* (Figure 1, c14-c21 and c1*-c4* in Table 1). This unexpected observation deserves further more detailed study.

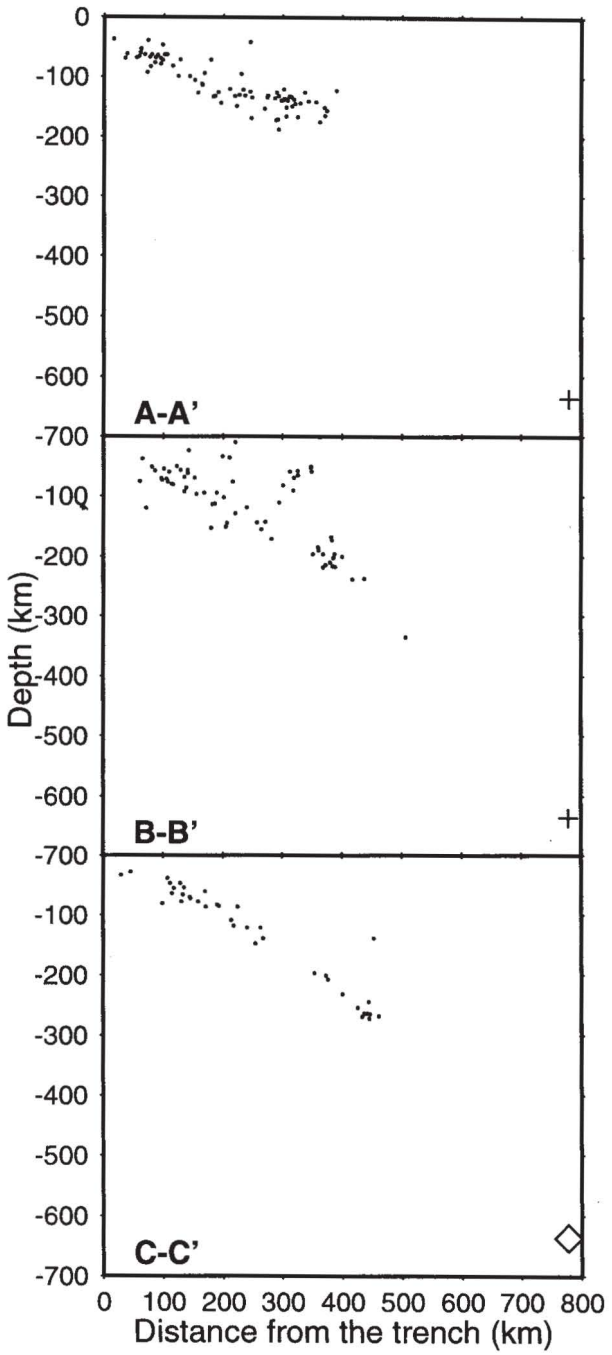

Fig. 5. Cross-sections A-A', B-B' and C-C' (40 km width, side view) of the Wadati-Benioff seismic zone of northern Chile. Open diamond is the Bolivian event of June 9, 1994. Crosses indicate the projection of the event of June 9, 1994 on the cross-sections A-A' and B-B'.

DISCUSSION AND CONCLUSION

A careful analysis has been attempted to retrieve new reliable estimates of D_m from the distribution of seismicity in different subduction zones. The values of A and V were found for each seismicity profile using the latest published data on the age of the ocean floor and the corrected global plate motion model NUVEL 1A (DeMets *et al.*, 1994). Corrections for the age of the subducted slab are introduced.

The data contain significantly smaller uncertainties of D_m and φ in comparison with previous studies. A general empirical dependence $D_m=f(\varphi)$ is obtained and compared with the modeled $D_m=f(\varphi)$ curves from Goto *et al.* (1983, 1985) and Spencer (1994) for T_{cr}=650°C. The models fit the empirical relation $D_m=f(\varphi)$ within the uncertainty limits for the range of D_m<240-260 km (quasi-linear section), and the better fit is obtained for the model of Spencer (1994). Prominent deviation of the general empirical dependence $D_m=f(\varphi)$ from the model curves in the range of φ from $20x10^2$ km to ~$35x10^2$ km is apparently the after-effect of equilibrium Ol-Sp phase transition which may be elevated up to depth of ~260 km within the relatively cold slab core.

To examine the influence of the Ol-Sp phase transition on D_m we compared the observed values of D_m and φ with the location of the corresponding "coldest" geotherms in the P-T phase diagram. Each geotherm has been estimated using the results of numerical modeling (Goto *et al.*, 1983, 1985) of the temperature distribution within the subducting slab with matching values of V, A and α. Approximate P-T conditions of the seismicity cutoff inside the cold core of the subducting slab were also obtained in a similar way applying the empirical fit $D_m=f(\varphi)$ for slightly extrapolated results of Spencer's (1994) model. For both models an apparent decrease of T_{cr} at the depth of ~190-270 km can be observed (Figure 2), which is in contradiction with the conclusions of several previous studies (e.g., Molnar *et al.*, 1979, Wortel, 1982). After a rough correction of the geotherms for the latent heat released by the equilibrium Ol-Sp phase transition (Figure 3), the seismicity cutoff temperature apparently remains at $T_{cr} \approx$ 650°C down to a depth of ~350 km. That result evidently relates observed upward deflection of the empirical dependence $D_m=f(\varphi)$ from the modeled curves to equilibrium Ol-Sp phase transition. The latent heat of the Ol-Sp transition increases the temperature within the slab, which partly delays a further increase of D_m in the range of $20x10^2$ km <φ<$35x10^2$ km (Figure 1).

The abrupt increase of D_m from ~260 km to > 600 km in the range of $35x10^2$ km < φ < $45x10^2$ km (Figure 1) can not be interpreted using the results of this study in favor of the deep seismicity being induced by the metastable Ol-Sp phase transition, although we cannot discard this reasonable mechanism. To approach this problem applying the empirical dependence $D_m=f(\varphi)$ an exceptionally accurate age estimates in other subduction zones and more adequate modeling are required.

The relatively low uncertainties in the estimates of D_m and φ allowed us to obtain the best approximating curve which can be used as a standard general dependence $D_m=f(\varphi)$ for studying the relation between convergence parameters and deep seismicity. Empirical $D_m=f(\varphi)$ curve is then applied formally to analyze the deep seismicity in the Chilean subduction zone and the Bolivian earthquake of June 9, 1994. Apparently the group of deep Chilean earthquakes south of 26°S occurred within the detached fragment of the slab. The examination of seismicity cross-sections in northern Chile subduction zone and the location of the corresponding D_m points on the $D_m=f(\varphi)$ plot imply that north of 23°S the deep events belong to the unfragmented subducting slab. The Bolivian earthquake of June 9, 1994 did not necessarily occur in the detached part of the slab. This event probably happened at the northernmost deep edge of the oldest segment of the subducted Nazca plate and represents a continuation of the deep seismicity cluster line of the northern Chile subduction zone.

ACKNOWLEDGMENTS

The authors thank R. Dmowska, C. Lomnitz, K. Michaelan, and J. Pacheco for attentive correction of the manuscript, D. Zhao for the seismic catalog of Japan, S. Cande for the discussion on the age estimates. The GMT-System software by P. Wessel and W. Smith was utilized in this study.

BIBLIOGRAPHY

AKAOGI, M., E. ITO and A. NAVROTSKY, 1989. Olivine-modified Spinel-Spinel Transitions in the System Mg_2SiO_4-Fe_2SiO_4: Calorimetric Measurements, Thermochemical Calculation, and Geophysical Application. *J. Geoph. Res., 94,* B11, 15671-15685.

ATWATER, T., 1989. Plate tectonic history of the northeast Pacific and western North America. *In:* The Eastern Pacific Ocean and Hawaii, The Geology of North America, edited by E.L. Winterer, D.M. Hussong, and R.W. Decker, v. N., pp. 21-71, Geol. Soc. of Am., Boulder, Co.

BEVINGTON, P.R., 1969. Data Reduction and Error Analysis for the Physical Sciences, 336 pp., McGraw-Hill, N.Y.

CIRCUM-PACIFIC COUNCIL FOR ENERGY AND MINERALS RESOURCES, 1981. Plate-Tectonic Map of the Circum-Pacific Region, Am. Assoc. Petrol. Geol., Tulsa, Okla.

DeMETS, C., R. G. GORDON, D. F. ARGUS and S. STEIN, 1994. Effects of recent revisions to the geomagnetic reversal time scale on estimates of current plate motions. *Geophys. Res. Lett., 21,* 2191-2194.

ENGEBRETSON, D. and S. KIRBY, 1992. Deep Nazca slab seismicity: Why is it so anomalous?, AGU 1992 Fall Meeting. EOS Trans. Am. Geophys. Un., 397.

FROHLICH, C., 1989. The nature of deep-focus earthquakes. *Ann. Rev. Earth Planet. Sci., 17,* 227-254.

GOTO, K., H. HAMAGUCHI and Z. SUZUKI, 1983. Distribution of stress in descending plate in special reference to intermediate and deep focus earthquakes. I. Characteristics of thermal stress distribution, *Tohoku*

Geophys. J. (The science reports of the Tohoku University, Series 5), 29, 81-105.

GOTO, K., H. HAMAGUCHI and Z. SUZUKI, 1985. Earthquake generating stresses in a descending slab. *Tectonophysics, 112,* 111-128.

GREEN, H. W., 1994. Solving the Paradox of deep earthquakes, Scientific American, 50-57.

GREEN, H. W. and P. C. BURNLEY, 1989. A new self-organizing mechanism for deep-focus earthquakes. *Nature, 341,* 733-737.

GREEN, H. W., T. E. YOUNG, D. WALKER and C. H. SCHOLZ, 1990. Anticrack associated faulting at very high pressure in natural olivine. *Nature, 348,* 720-722.

KALININ, V. A. and M. V. RODKIN, 1982. Physical model for the source of deep focus earthquakes. *Izv. Acad. Sci. USSR Geophys., 8,* 3-12.

KIRBY, S. H., E. A. OKAL and E. R. ENGDAHL, 1995. The 9 June 94 Bolivian earthquake: An exceptional event in an extraordinary subduction zone. *Geophys. Res. Lett., 22,* 2233-2236.

KIRBY, S., W. B. DURHAM and L. A. STERN, 1991. Mantle phase changes and deep-earthquake faulting in subduction lithosphere. *Science, 252,* 216-225.

KLITGORD, K. and J. MAMMERICKX, 1982. East Pacific rise: Magnetic anomaly and bathymetric framework. *J. Geophys. Res., 87,* 6725-6750.

KOSTOGLODOV, V. V., 1989. Maximum depth of earthquakes and phase transformation within the lithospheric slab descending in the mantle. *In:* Physics and Interior Structure of the Earth, edited by V. A. Magnitsky, Nauka, Moscow.

KOSTOGLODOV, V., 1994. Structure and seismotectonic segmentation of Chilean subduction zone, 7o Congreso Geológico Chileno 1994, Concepción, 17-20 Oct. 1994, Univ. de Concepción, Actas Volumen II, 1383-1387.

KOSTOGLODOV, V. and W. BANDY, 1995. Seismotectonic constraints on the convergence rate between the Rivera and North American plates. *J. Geophys. Res., 100,* 17,977-17,989.

LARSON, R. L., W. C. PITMAN III, X. GOLOVCHENCO, C. S. CANDE, J. F. DEWEY, W. F. HAXBY and J.L. LaBRECQUE, 1985. The Bedrock Geology of the World, Freeman and Co., New York.

LARUE, B. M., J. DANIEL, C. JOUANNIC and J. RECY, 1977. The South Rennel trough: evidence for a fossil spreading zone. *In:* International Symposium on Geodynamics in South-West Pacific, Noumea, 1976., pp. 51-62, Editions Technip, Paris.

LAY, T., 1994. Seismological constraints on the velocity structure and fate of subducting lithospheric slabs: 25 years of progress. *Advances in Geophysics, 35,* 1-185.

LUNDGREN, P. and D. GIARDINI, 1995. The June 9 Bolivia and March 9 Fiji deep earthquakes of 1994: I. Source processes. *Geophys. Res. Lett., 22,* 2241-2244.

MAMMERICKX, J., 1984. The morphology of propagating spreading ridges. *J. Geophys. Res., 89,* 1817-1828.

MAMMERICKX, J. and K. KLITGORD, 1982. Northern East Pacific rise: evolution from 25 m.y. B.P. to the present. *J. Geophys. Res., 87,* 6751-6759.

MAMMERICKX, J., D. F. NAAR and R. L. TYCE, 1988. The Mathematician paleoplate. *J. Geophys. Res., 93,* 3025-3040.

MAYES, C. L., L. A. LAWVER and D. T. SANDWELL, 1990, Tectonic history and new isochron chart of the South Pacific. *J. Geophys. Res., 95,* 8543-8567.

McKENZIE, D. P., 1969. Speculations on the consequence and cause of plate motions. *Geophys. J. R. Astron. Soc., 18,* 1-32.

McKENZIE, D. P., 1970. Temperature and potential temperature beneath island arcs. *Tectonophysics, 10,* 357-366.

MEADE, C. and R. JEANLOZ, 1991. Deep-Focus earthquakes and recycling of water into the Earth's Mantle. *Science, 252,* 68-72.

MOLNAR, P., D. FREEDMAN and J. S. SHIH, 1979. Length of intermediate and deep seismic zones and temperatures in downgoing slabs of lithosphere. *Geophys. J. R. Astron. Soc., 56,* 41-54.

MUELLER, R. D., W. R. ROEST, J.-Y. ROYER, L. M. GAHAGAN and J. G. SCLATER, 1993. A digital age map of the oceanic floor. SIO Reference Series No. 93-30, Scripps Inst. of Oceanography, Univ. of California at San Diego, La Jolla, Ca.

NAKANISHI, M., K. TAMAKI and K. KOBAYASHI, 1992. Magnetic anomaly lineations from Late Jurassic to Early Cretaceous in the west-central Pacific Ocean. *Geophys. J. Int., 109,* 701-719.

NEPROCHNOV, Y. N., L. R. MERKLIN and A. A. SHREYDER, 1979. New data on the structure and geomagnetic field of the Sunda (Java) trench. *Oceanology, Acad. Sci. USSR, Engl. Transl., 19,* 3, 281-283.

PARDO, M. and G. SUAREZ, 1993. Steep subduction geometry of the Rivera plate beneath the Jalisco block in Western Mexico. *Geophys. Res. Lett., 20*, 2391-2394.

PARDO, M. and G. SUAREZ, 1995. Shape of the subducted Rivera and Cocos plates in Southern Mexico: Seismic and Tectonic implications. *J. Geophys. Res., 100, B5*, 12357-12373.

RENKIN, M. L. and J. G. SCLATER, 1988. Depth and age in the North Pacific. *J. Geophys. Res., 93*, 2919-2935.

SHIONO, K. and N. SUGI, 1985. Life of an oceanic plate: cooling time and assimilation time. *Tectonophysics, 112*, 35-50.

SPENCER, J. E., 1994. A numerical assessment of slab strength during high- and low-angle subduction and implications for Laramide orogenesis. *J. Geophys. Res., 99*, 9227-9236.

SUNG, C. M. and R. G. BURNS, 1976. Kinetics of high-pressure phase transformations: implications to the evolution of the olivine-spinel transition in the downgoing lithosphere and its consequences on the dynamics of the mantle. *Tectonophysics, 31*, 1-32.

SYKES, L., 1966. The seismicity and deep structure of island arcs. *J. Geophys. Res., 71*, 2981-3006.

TURCOTTE, D. L. and G. SCHUBERT. Structure of the Olivine-Spinel phase boundary in the descending lithosphere. *J. Geophys. Res., 76*, 7980-7987.

VON HERZEN, R. P., 1967. Heat flow and some implications for the mantle. *In:* The Earth's Mantle, edited by T.G. Gaskell, pp. 197-230, Academic, N.Y.

WEISSEL, J. K., A. B. WATTS and A. LAPOUILLE, 1982. Evidence for late Paleocene to late Eocene seafloor in the southern New Hebrides basin. *Tectonophysics, 87*, 243-2251.

ZHAO, D., A. HASEGAWA and S. HORIUCHI, 1992. Tomographic imaging of P and S wave velocity structure beneath northeastern Japan. *J. Geophys. Res., 97*, 19909-19928.

A. Gorbatov[1], V. Kostoglodov[1] and E. Burov[2]
[1] *Instituto de Geofísica, Universidad Nacional Autónoma de México, 04510 México D.F., México.*
[2] *Institut de Physique du Globe de Paris, 75252 Paris, CEDEX 05, France.*